



Exploring the Interaction of Oligonucleotides with Single-Walled Carbon Nanotube as industrial bio-catalysis: A Molecular Dynamics Simulation Study

Maryam Ghanbari-Ghanbarlo, Mohammad Reza Bozorgmehr*, Ali Morsali

Department of Chemistry, Mashhad Branch, Islamic Azad University, Mashhad, Iran

* E-mail: bozorgmehr@mshdiau.ac.ir (mr_bozorgmehr@yahoo.com)

Received 23 July 2023; accepted 5 September 2023

Abstract

In this research, the interaction of four single stranded nucleic acid homopolymers including hemo deca adenine, dA10, hemo deca thymine, dT10, hemo deca guanine, dG10 and hemo deca cytosine, dC10, with single-walled carbon nanotubes was studied by molecular dynamics simulation method. The simulations were performed using Gromacs software and Amber force field, with a simulation time of 250 nanoseconds and 2 femtosecond time step. The root mean square deviation (RMSD) values were calculated to validate the simulations, indicating that the systems reached equilibrium. The distance between the center of mass of the hemo deca polymers and the surface of the carbon nanotube was also calculated, and the results showed that the interaction of monocyclic organic bases with the nanotubes was higher due to less steric hindrance with the phosphate group. The results suggest that monocyclic organic bases may be more suitable for interactions with carbon nanotubes due to their lower steric hindrance.

Keywords: *Nanotube, Biosensor, Detection, Organic base, Polymer*

1. Introduction

Biosensors are analytical devices that have the ability to detect and quantify the presence of biological or chemical substances [1]. Also, biosensors can be used as biocatalysts [2]. They are based on the principle of specific recognition of the target analyte by a biological recognition element, such as enzymes, antibodies, or nucleic acids. Biosensors can be used in various fields, such as medical diagnosis, environmental monitoring, food analysis, and drug discovery [3]. The development of biosensors has been driven by the need for rapid and accurate detection of various analytes, especially in clinical settings. Traditional methods of detection, such as chromatography and spectrophotometry, are time-consuming, require specialized skills, and are often not suitable for on-site analysis [4]. Biosensors, on the other hand, offer several advantages, including rapid detection, portability, ease of use, and the ability to monitor analytes in real-time [5]. The design and development of biosensors depend on the specific application and the type of analyte to be detected. Biosensors can be classified based on the type of biological recognition element, the transduction mechanism, and the type of matrix or support. For example, electrochemical biosensors use electrochemical transduction to convert the biological recognition event into an electrical signal, while optical biosensors use optical properties, such as fluorescence or absorbance, to detect the analyte [6].

Gaining knowledge from specific biochemical interactions has both theoretical and practical

applications. Biosensors are crucial in quantifying and identifying such interactions as they can detect and convert them into visible signals [7]. The biosensor consists of two parts: the identifier, which selectively interacts with the analyte, and the converter, which converts the interaction into a signal [8]. To be effective, biosensors must be smaller than the bioanalyte to avoid interfering with its behavior. Nanowires, quantum dots, nanoparticles, graphene, and carbon nanotubes are suitable for preparing the converter portion of miniature biosensors [9]. Carbon nanotubes are particularly advantageous due to their unique chemical, physical, and electrical properties. Carbon nanotube-based biosensors have been used to identify bacteria, glucose, viruses, gases, and chemical compounds. The biosensor identification unit typically comprises antibodies, aptamers, lectins, or nucleic acid sequences. Selective interaction with the analyte is crucial, and single-stranded nucleic acid complexes and carbon nanotubes have high selectivity [10].

Theoretical studies have shown that single-stranded nucleic acids in solution interact with carbon nanotubes and penetrate into them [11]. The stability of these structures depends on the homo- or hetero-oligomer and the length of the carbon nanotube. Peptide interactions play a crucial role in the interaction of single-stranded nucleic acids with carbon nanotubes. UV-visible spectroscopy has shown that cytosine homo-polymer has the highest interaction, and guanine homo-polymer has the least interaction with carbon nanotubes [12].

Despite the studies on the interaction between nucleic acids and carbon nanotubes, the mechanism of interaction is not well understood [13]. In this study molecular dynamics simulations have been used to investigate the interaction of some homo-polymers of bases constructing nucleic acid with carbon nanotubes.

2- Method

The structure of basic organic bases to form homopolymers is shown in Figure 1.

Because the force field parameters for nucleic acids are available by default, optimization of the above structures was done using Gromacs 5.1.2 [15]. A chiral nanotube structure (6, 5) with a diameter of 7.46 angstroms

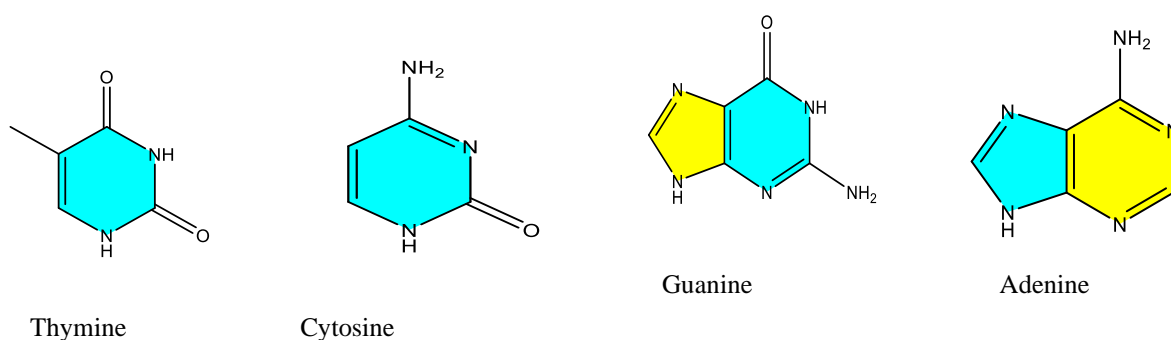


Fig. 1 Structure of organic bases adenine, guanine, cytosine and thymine

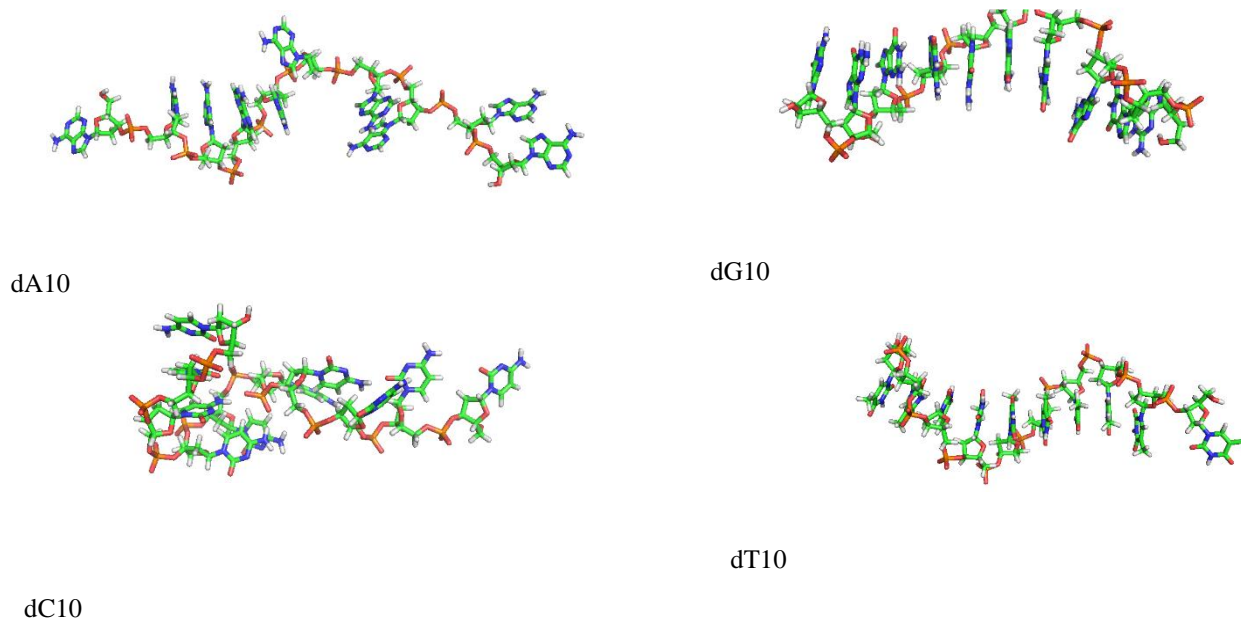


Fig. 2 Spatial structure of homo deca polymers designed from nucleotide bases adenine, guanine, cytosine and thymine

was designed. Since the force field parameters of carbon nanotubes are not available by default in Gromacs software, Ambergtools software was used to determine these parameters [16]. Optimum structure of nanotubes is needed to use Ambergtools. The structure of this nanotube was optimized using B3LYP density functional theory method and 6-31G basis function. Gaussian 09 software was used to perform quantum calculations [17]. The designed nanotube structure is shown in Figure 3.

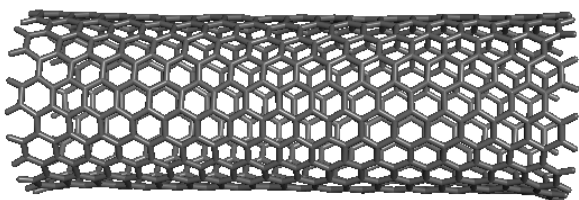


Fig. 3 Optimize designed structure of carbon nanotube

The length of this nanotube was considered to be 83.1 angstroms, which is slightly larger than the length of the designed homo deca polymers. Based on the structures designed for homo deca polymers and carbon nanotubes, four simulation boxes were designed. Carbon nanotubes were placed in the center of these boxes. Then, each homo deca polymer was randomly placed in the simulation boxes. Then, each of the simulation boxes was filled by TIP3P model waters [18] that are consistent with the Amber force field. Since nucleotide phosphate groups have a negative charge, nine sodium ions were added to each of the simulation boxes for neutralization. The steepest descent algorithm was used to minimize the energy of the designed systems. Then, each of the designed systems reached equilibrium in two steps in NVT and NPT ensemble. In the final step, the simulation was performed for 250 nanoseconds with a step of 2 femtoseconds for each of the designed systems. V-rescale and Berendsen algorithms were used to control the pressure and temperature of the system [19]. Molecular dynamics simulation calculations were performed with Amber force field and Gromacs software version 5.1.2.

3-Results and discussion

To control the appropriateness of the simulation time, the root mean square deviation (RMSD) value of each of the designed systems was calculated. The obtained values are shown in Figure 4.

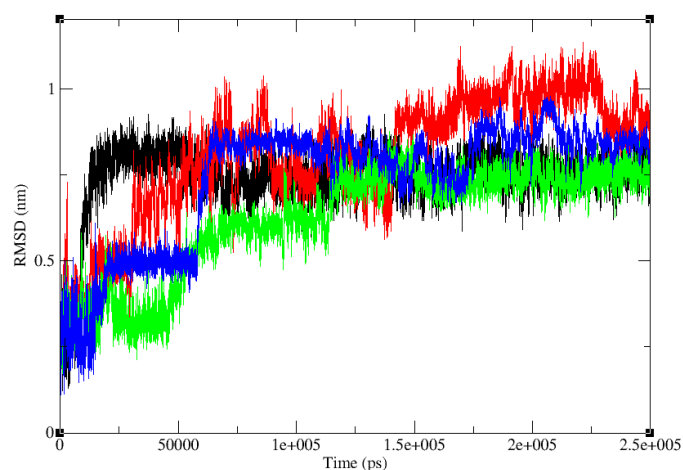


Fig. 4 RMSD values for dA10 (black), dC10 (red), dG10 (green) and dT10 (blue)

According to the figure, it can be seen that the designed systems have reached equilibrium. In fact, the range of RMSD changes is between 0.2 and 1.2 nm, which is not much for the system with this specific number of atoms, and the observed fluctuations are not considered a large deviation from equilibrium. However, it can be seen that the fluctuations related to dC10 and dG10 have the highest and lowest values, respectively. Since the geometric parameters play a large role in the structure and performance of the nucleic acid-nanotube complex, the distance between the center of mass of this homo deca polymers and the surface of the carbon nanotube was calculated during the simulation for the designed systems. In the figure below, the schematic of this distance in 50 nanoseconds is shown for the dG10 system:

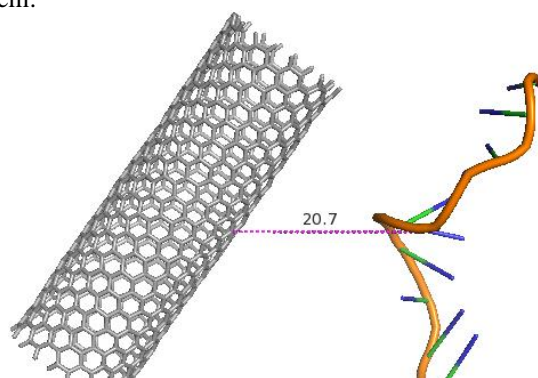


Fig. 5 Schematic of the center of mass distance of carbon nanotube and dG10 in 50 nanoseconds

Similarly, this distance was calculated for all designed systems, and the results are shown in the figure below. In obtaining these figures, it is necessary to determine the center of mass of the homo deca polymer. For this purpose, a Python script was written that receives the

coordinates of the atoms involved in the simulation as input and calculates the coordinates of the center of mass.

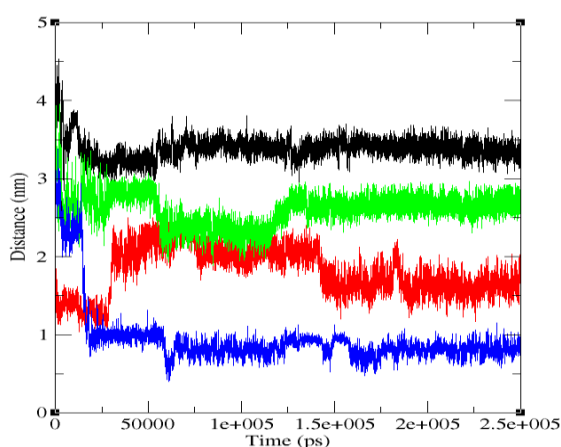


Fig. 6 The values of the distance between the center of mass of homo deca polymer and the carbon nanotube surface, dA10 (black), dC10 (red), dG10 (green) and dT10 (blue)

According to the figure, it can be seen that the distance calculated for all systems fluctuates around 150 nanoseconds until the time of simulation, and then this distance changes around an equilibrium value. The lowest and highest values of the distance calculated are related to homo deca polymer dT10 and dA10, respectively. Also, this distance is greater for homo deca polymers that have purine organic base (bicyclic base) than homo deca polymers that have pyrimidine organic base (monocyclic base). Since the binding of homo deca polymer to carbon nanotubes requires the orientation of organic bases so that they can interact with benzene rings in the structure of nanotubes π - π , therefore the bases must rotate around the glycosidic bond with sugar. On the other hand, the rotation of these bases leads to steric hindrance with the phosphate group. Therefore, the interaction of monocyclic organic bases with nanotubes has been higher. This matter can be proven in the lower distance of these homo deca polymers in the figure above

4-Conclusion

In conclusion, an in silico study was conducted to investigate the interaction between homo deca polymers and carbon nanotubes. Molecular dynamics simulations were performed using Gromacs software and Amber force field with a simulation time of 250 nanoseconds. The simulations were validated by calculating the root mean square deviation (RMSD) values, which indicated that the systems reached equilibrium. The distance between the center of mass of the homo deca polymers and the surface of the carbon nanotube was also calculated during the simulation. The results showed that the distance fluctuated around an equilibrium value, and the lowest and highest values were related to homo deca polymer dT10 and dA10, respectively. Moreover, it was observed that the interaction of monocyclic organic bases with the nanotubes was higher due to less steric hindrance with the phosphate group. Overall, this study provides insights into the behavior of nucleic acid-nanotube complexes and can be beneficial in designing new nanomaterials for various applications.

References

- [1] H. Sohrabi, A. Hemmati, MR. Majidi, S. Eyvazi, A. Jahanban-Esfahlan, B. Baradaran, *Trend in Anal. Chem.* 143 (2021) 116344.
- [2] KA. Maqdai, M. Alzhamly, HM. Iqbal, I. Shah, SS. Asghraf, *Nanomaterials*, 11 (2021) 1460.
- [3] P. Mehrotra, *J. Oral Biol. Cran. Res.* 6 (2016) 153.
- [4] R. Monosik, M. Stredansky, E. Sturdik, *Acta chimica slovacica*, 5 (2012) 109.
- [5] S. Vigneshvar, C. Sudhakumari, B. Senthilkumaran, H. Prakash, *Frontiers in bioeng. biotech.* 4 (2016) 11.
- [6] A. Haleem, M. Javaid, RP. Singh, R. Suman, S. Rab, *Sens. Int.* 2 (2021) 100.
- [7] X. Guo, *Adv. Mat.* 25 (2013) 3397
- [8] X. Huang, Y. Zhu, E. Kianfar, *J. Mat. Res. Tech.* 12 (2021) 1649.
- [9] K. Malecka-Baturo, *MDPI*, 1 (2022) 1052.
- [10] S. Kruss, AJ. Hilmer, J. Ahang, NF, Reuel, B. Mu, *adv. Drug Del. Rev.* 65 (2013) 1933.
- [11] I. Yeh, G. Hummer, *Proc. Nat. Acad. Sci.* 10 (2004) 12177.
- [12] D. Roxbury, J. Mittal, A. Jagota, *Nano Lett.* 12 (2012) 1464.

- [13] S. Gowtham, RH. Scheicher, R. Pandey, SP. Karna, R. Ahuja, *Nanotech.* 19 (2008) 125701.
- [14] WL. Delano, *San. Carl.* 1 (2004) 68.
- [15] H. Berendsen, D. Spoel, R. Drunen, *Comp. Phys. Comm.* 91 (1995) 43.
- [16] RM Betz, RC. Walker, *J. Comp. Chem.* 36 (2015) 79.
- [17] M. Frisch, F. Clemente, *Gaussian*, 20 (2009) 44.
- [18] P. Mark, L. Nilsson, *J. Phys. Chem.* 105 (2001) 9954.
- [19] Q. Ke, X. Gong, S. Liao, C. Duan, L. Li, *J. Mol. Liq.* 365 (2022) 120116.